Proceedings of the 21st ICSMGE, Vienna, Austria, 14 – 19 June 2026. Pistrol, Adam & Schweiger (eds.)
Published by: ÖGG, Austrian Society for Geomechanics, Salzburg, Austria, ISBN 978-3-9503898-4-5
https://doi.org/10.53243/ICSMGE2026-815

Three-dimensional FE analysis of twin-tunnels excavation in green-field conditions

Luca Masini, Sebastiano Rampello
Dept. of Geotechnical and Structural Engineering, University of Rome Sapienza, Rome, Italy, luca.masini@uniroma1.it

Francesco D'Annunzio
Italferr S.p.a., Rome, Italy

ABSTRACT: The construction of the Line C of Rome underground entailed the use of two earth-pressure balance machines (EPBMs) to excavate the twin tunnels within the historic city centre. The objective was to minimise any potentially detrimental interferences with existing monuments and buildings of historical value. This resulted in the implementation of an extensive monitoring programme, the objective of which was to evaluate the impact of the Line C on the surrounding monuments. Furthermore, this programme provided invaluable opportunities for field investigation of the ground response. This paper presents the results of a three-dimensional finite element (FE) analysis conducted to simulate the excavation of the Line C twin tunnels beneath a green-field instrumented research site close to the Basilica of San Giovanni. A constitutive model capable of describing the non-linear and inelastic soil behaviour since the beginning of the loading paths was adopted, using the same set of constitutive model parameters which were calibrated on the results of a detailed geotechnical characterisation of the site and which have been shown to successfully simulate the observed behaviour of deep excavations carried out in the same area. The results of the analyses were found to reproduce satisfactorily the observed displacement field induced by the excavation of the twin tunnels. The comparison between the observed and predicted behaviour highlighted the potential for numerical analyses, despite being performed with widely used tools, to be profitably used to predict the performance of complex geotechnical problems, provided that the adopted constitutive model is carefully calibrated on laboratory and site investigations.

KEYWORDS: 3D Numerical analyses, case history, ground movements.

1 INTRODUCTION

Line C of the Rome Underground is the city's third line. Once fully operational, it will improve connections to the south-eastern suburbs, reducing traffic congestion in the city centre. The central section of the route presented an impressive engineering challenge as it was excavated in the historic city centre, close to many monuments from the Roman era, of invaluable archaeological and historical value. To minimise ground movement during construction, two earth pressure balance machines (EPBMs) excavated the twin-bore tunnels from the shield insertion pit close to San Giovanni's Square to the future Venezia station. Despite remarkable research and recent improvements in EPBM excavation techniques, tunnelling still causes movement in the surrounding soil. Therefore, accurate prediction of ground settlements remains one of the most challenging aspects of geotechnical engineering. In light of this, a substantial monitoring programme was implemented during the construction of Line C to evaluate the impact on historical heritage and adopt advanced mitigation techniques for any potential adverse effects.

This paper presents the results of surface and subsurface monitoring related to the excavation of the twin-bore tunnels at an instrumented research site. The test site reproduced greenfield conditions, as there were no pre-existing structures nearby. The observed response patterns are compared with the computed behaviour obtained from 3D finite-element (FE) analyses, which simulated the progressive advance of the tunnel face.

2 THE METRO C GREEN-FIELD SITE

A fully instrumented green field control section was installed between San Giovanni and Amba Aradam/Ipponio stations to control the performance of the two EPB-TBMs in ground conditions representative of those encountered throughout contract T3. The two tunnels were excavated from Multifunctional Shaft 3.3 towards Amba Aradam/Ipponio station. The southbound tunnel was excavated approximately 18 days after completion of the northbound tunnel (Masini et al., 2020; 2021a). The tunnel axes are spaced approximately 13 to 18 metres apart, with a depth z_0 = 26 m below ground level. The two EPB TBMs that excavated the Metro C tunnels have a maximum cutterhead diameter of 6.71 m and a tapered shield length of 11.8 m, with the shield diameter reducing from 6.69 m behind the rotating head to 6.67 m at the tail. This results in an annular gap that increases from 10 mm to 20 mm towards the shield tail. Conventional bolted precast concrete segmental lining rings with a nominal length of 1400 mm were erected within the shield body. These have an inner and outer diameter of 6.1 m and 6.4 m, respectively, i.e. a ring thickness of 0.3 m. The resulting tail void gap of 155 mm between the tunnel lining extrados and the excavated ground was filled using a two-part grout injection system.

Figure 1 shows a plan view of the MON05 greenfield array of instruments. Seventeen boreholes were excavated, each one housing one instrument for subsurface monitoring. Specifically, five vibrating wire piezometers, five inclinometer casings and seven Trivec casings (Köppel et al., 1983) were installed. The latter allow the three orthogonal components of displacement to be measured at 0.5 m depth intervals. Five Trivec casings and three inclinometer casings extend approximately one tunnel diameter (33–34 metres) below ground level. One Trivec casing and one inclinometer casing were installed at the centre of each tunnel, with the toe of the casings positioned approximately 3 m above the tunnel crown. An optical prism was installed at the top of each borehole to obtain absolute subsurface settlement profiles. Ground surface settlements were measured by precise levelling of 33 surface monitoring points (SMPs).

Changes in pore water pressure induced by tunnelling near the tunnels were measured using five vibrating wire piezometers installed in the layer of fine-grained soil.

Figure 2 shows a geotechnical cross-section of the site based on the site investigation campaigns carried out between 1995 and 2011. First encountered from the nearly horizontal ground surface, at 35 m above sea level (a.s.l.), is an 18 m-thick layer of heterogeneous made ground (MG), consisting mainly of coarse-grained sand and gravel. Underneath this, recent alluvial deposits of the Tiber River extend to a depth of 30 m. Specifically, organic clayey silts (LSO) are mostly found at the

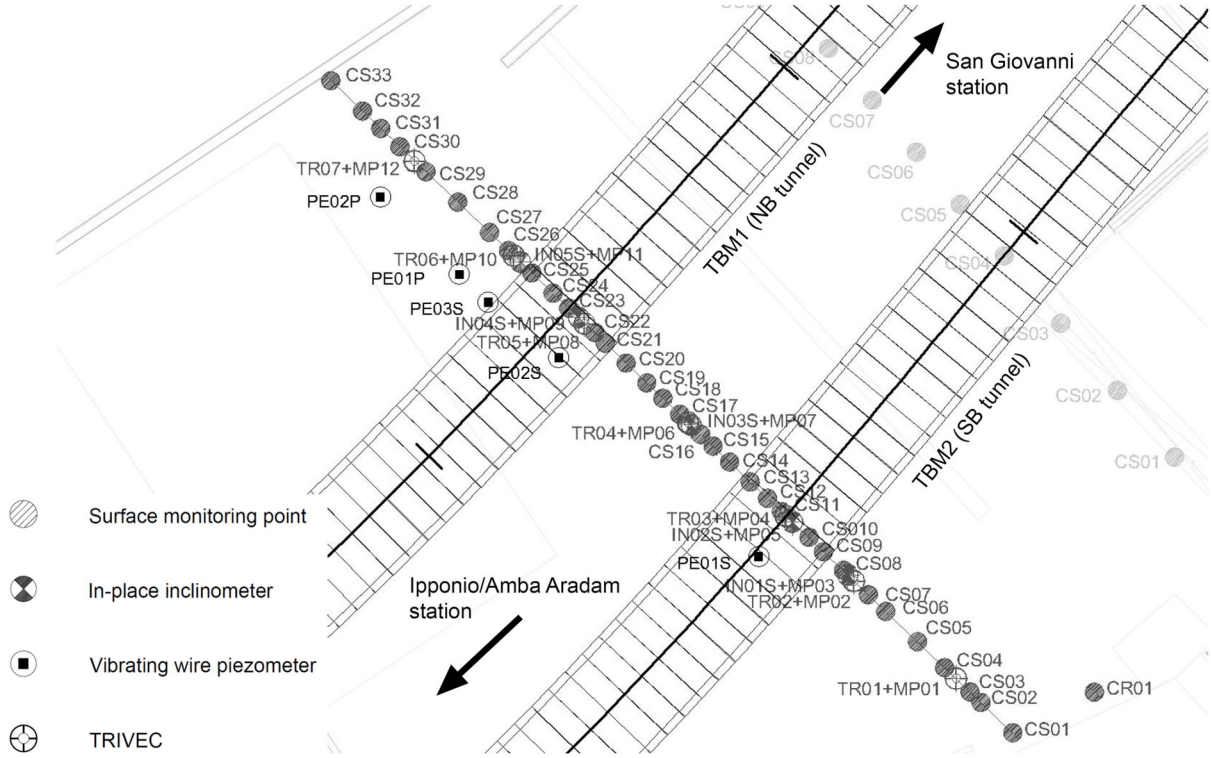

Figure 1. Instrumentation layout (plan view) of the MON05 greenfield monitoring array.

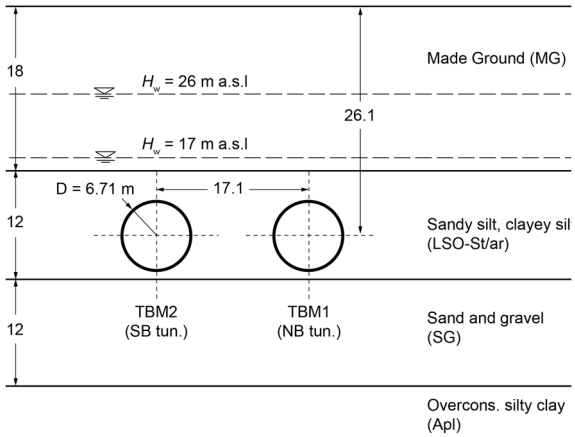

Figure 2. Instrumentation layout (plan view) of the MON05 greenfield monitoring array.

top of sandy and clayey silts (St/Ar), with an overall thickness of approximately 12 m. These overlie a 12-metre-thick layer of sand and gravel (SG), extending to a depth of 42 m, which is then followed by a thick layer of stiff, overconsolidated silty clay (Apl). The alluvial soils vary in grading but have similar physical and mechanical characteristics. The tunnels were excavated in the fine-grained LSO and St/Ar soils.

The pore water pressure regime at the site is characterised by downward seepage in the silty soils from the made ground, where a constant hydraulic head of 26 m a.s.l. was measured, to the deep layer of sandy gravel at a constant head of 17 m a.s.l.

3 3D FE MODEL

Figure 3a shows the 3D finite element (FE) model used for the back-analysis of the observed displacement field induced by tunnelling. The model represents a soil volume measuring 150 m in width, 42 m in height and 190 m in length. The base of the mesh is located at the bottom of the sandy gravel (SG), 42 m below ground level. The greenfield monitoring section is situated approximately halfway along the 160 m tunnel path. Standard fixities were applied along the mesh boundaries. In the numerical model, the actual path of both tunnels (Figure 3b) is reproduced, with the tunnel axes located at a depth z_0 = 26.1 m and an axis-to-axis horizontal distance of 17.1 m at the greenfield monitoring section MON05. The same FE model was also used to assess the efficiency of an embedded barrier (depicted in Fig.3b) to mitigate the effects of tunnelling. However, for the sake of brevity, this paper focuses on the results obtained at the position of MON05 array, without the beneficial effects of the barrier.

The analyses were carried out using PLAXIS 3D code (Brinkgreve et al., 2013). The mechanical behaviour of the made ground (MG) and sandy gravel (SG) layers, which were characterised primarily via in situ tests, was described using the Hardening Soil (HS) model (Schanz et al. 1999). The behaviour of the recent alluvial soil (LSO/St-Ar), for which accurate laboratory test results were available (Rampello et al., 2019), was described using the Hardening Soil model with small-strain stiffness (HSsmall). This is a combination of the HS model proposed by Schanz et al. (1999) and the elastic small-strain model developed by Benz et al. (2009). Along with the same features as the HS model, the HSsmall model has the advantage of describing the hysteretic soil behaviour at very small strains introducing the initial shear modulus G_0 and the decay of the secant shear stiffness ratio G_s/G_0 with shear strain γ. The strength and stiffness parameters of the soils were calibrated against triaxial tests carried out with local axial strain transducers, and resonant column tests, while the profile of small-strain shear modulus was calibrated against in situ cross-hole tests. Table 1 lists the input parameters adopted in the analyses. The FE analyses were carried out in terms of effective stresses assuming drained behaviour for the soils interacting with tunnel excavation, of high-to-medium permeability, and the tunnel lining as impervious.

Table 1. Soils parameters.

Soil layer	γ (kN/m^3)	ν (-)	c' (kPa)	φ' (°)	OCR (-)	K_0 (-)	G_0^{ref} (MPa)	$\gamma_{0.7}$ (%)	E_{ur}^{ref} (MPa)	m (-)	$E_{ur}^{ref}/E_{50}^{ref}$ (-)	$E_{50}^{ref}/E_{oed}^{ref}$ (-)
MG	17	0.2	5	34	3.5	0.441	-	-	240	1	10	1
LSO	19.5	0.2	28	27	1.3	0.62	125	0.035	150	0.8	18	1.5
SG	20	0.2	0.1	40	7.5	0.36	-	-	900	0.4	10	1

The lithostatic stress state was initially set by reproducing the observed downward stationary seepage through the fine-grained soils (LSO, St/Ar units).

The EPBM tunnel excavation process was divided into several construction stages.

The same steps were repeated for each stage to simulate the support pressure at the tunnel face, the tapering shape of the TBM shield, the excavation of the soil, the installation of the tunnel lining, and the grouting of the gap between the soil and the newly installed lining (Broere & Brinkgreve, 2002). The 11.2 m shield, equivalent to eight tunnel rings, was modelled using 0.03 m thick shell elements with a diameter of D = 6.4 m, a Young's modulus E = 210 GPa, and a Poisson's ratio ν = 0.15. The overcutting at the rotating head and the tapering of the TBM body were modelled by applying a linear contraction to the shield's shell elements, increasing from 0% at the head to 0.55% at the tail. This value was calibrated to match the volume loss measured at ground surface after completion of the northbound tunnel, the first to be excavated, and was also adopted for the southbound tunnel. The weight of the shell elements (γ = 90 kN/m³) includes the weight of the machinery enclosed within the shield, as well as the weight of the spoil within the excavation chamber. The final concrete lining, installed 1 ring away behind the shield, was modelled as a 0.3 m thick continuous ring with an inner diameter of 6.4 m. This was done using solid elements with a unit weight γ = 25 kN/m³, a Young's modulus E = 30 GPa, and a Poisson's ratio ν = 0.2. Purely frictional interface elements were used at the soil–shield and soil–lining contacts, with the angle of shearing resistance of the adjacent soil reduced by a coefficient R_{int} = 0.7. Face support pressure and pressurised backfill injection were modelled as distributed loads, linearly increasing with depth. The former was applied to the soil at the face of the excavation, while the latter at the intermediate zone between the shield and the permanent lining. The values adopted for both tunnels were obtained as the average values of those measured at the test site by the TBM contractor.

Tunnelling is modelled in discrete steps, removing one slice of soil (1.4 m) and advancing the support pressure, shield and lining by an equal length from one side of the mesh to the other, for a total path of 160 m.

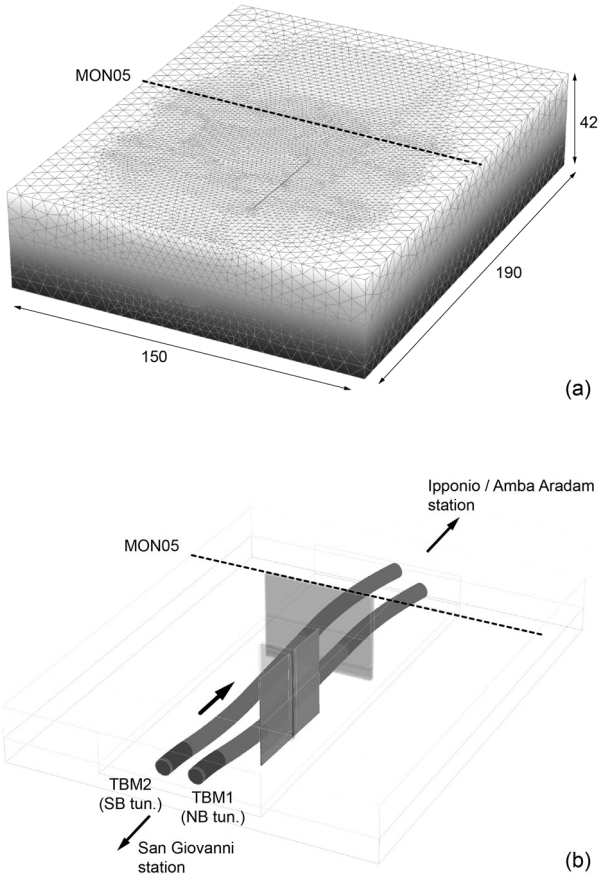

Figure 3. 3D FE model: (a) mesh and (b) path of the tunnels.

4 ANALYSIS RESULTS AND COMPARISON WITH FIELD DATA

The northbound tunnel (TBM1) was excavated first, followed by the south tunnel (TBM2). The results presented below refer to the passage of both TBMs.

Figure 4 shows the observed transverse settlement profile at ground level after the second TBM has passed. The results of the finite element simulation, also plotted in the figure, are seen to be in a good agreement with the monitoring data from the SMPs. The maximum settlement (w = 8.25 mm) was measured closer to the TBM1 axis (7.37 m). The northern-half trough, where TBM1 is located, has a larger width than the southern-half trough. The corresponding trough width parameters are K = 0.54 and K = 0.64, respectively. This is most likely due to the soil on the northern side being disturbed and softened by the passage of TBM1. The estimated volume losses were 0.39% for the southern half and 0.47% for the northern half of the trough;

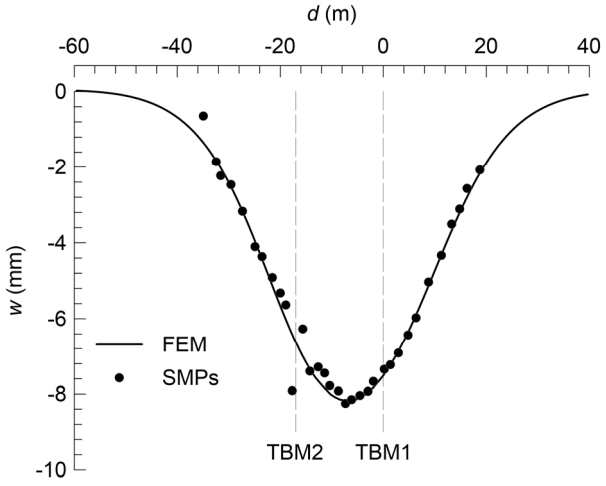

Figure 4. Ground surface settlement due to southbound tunnel excavation.

both are larger than the volume loss computed for the passage of TBM1 (0.30%). As the TBM operating parameters were similar for TBM1 and TBM2, it can be concluded that the higher volume loss induced by TBM2 is due to softening of the ground induced by the excavation of the first tunnel.

Figure 5 shows a comparison of the observed and computed subsurface settlement troughs at various depths following the completion of both tunnels. Distances are referred to the axis of the northbound tunnel (TBM1). The settlement troughs were observed to be asymmetric, with larger settlements observed slightly closer to TBM2. At the shallowest depth (z = 4 m), the maximum cumulative settlement (w = 7.7 mm) occurred between the centre lines of the tunnels. Conversely, data measured from the Trivec casing TR04 at deeper points showed smaller displacements than those provided by the two adjacent Trivec casings, installed closely above the tunnels. This behaviour differs from that commonly observed during the excavation of twin tunnels, as reported by Wan et al. (2017), where the maximum displacement typically occurs between the tunnels. This suggests that errors may have affected the deeper readings obtained from the TR04 casing and that greater displacements actually occurred between the tunnels. This observation is corroborated by the numerical results showing that the location of maximum settlement is always between the tunnels. Specifically, the maximum settlement occurs closer to the TBM1 axis (6.92 m) at shallower depths, moving towards the TBM2 axis as the depth increases. For z = 16 m, the maximum settlement (w = 9.4 mm) was computed at a distance of 7.24 m from the TBM2 axis and 9.76 m from the TBM1 axis.

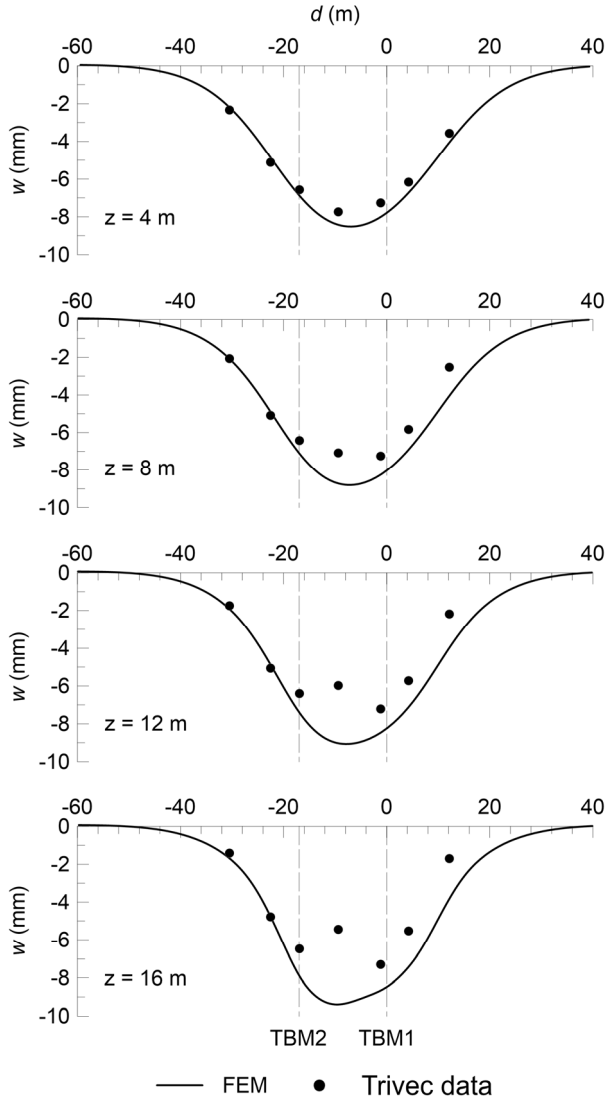

Figure 5. Subsurface settlement profiles.

Figure 6 shows the profiles of the cumulative vertical displacement provided by the Trivec casings along the MON05 array after the TBM2 had fully passed. Negative y-axis values indicate settlement. As expected, the displacements decrease with increasing distance from the TBM2 axis. However, none of the alignments can be considered outside the zone of influence of TBM2, as the effects of the southbound tunnel excavation extended to the location of Trivec TR07 (about 29 m away from the TBM2 axis), where the measured ground surface settlement increased from approximately 2 mm after the passage of TBM1 (not shown here for brevity) to slightly less than 4 mm, due to the soil being softened by the excavation of the first tunnel. Conversely, the maximum settlement measured from Trivec TR01, which is located 13.52 m from the TBM1 axis and approximately 31 m from the TBM2 axis, was only 2.5 mm (approximately 64% of the maximum value measured by Trivec TR07).

At the lowest measuring point of Trivec TR03, which is 2.65 m above the TBM2 crown, the maximum measured settlement was 7.6 mm. No heave was detected below the tunnel spring line by Trivec TR04, which is located between the tunnels, or by Trivec TR02, which is installed about 4.5 m away from the southbound tunnel axis. However, a maximum heave of 1.6 mm was observed at approximately the crown level from Trivec TR06, which is about 21 m away from the southbound tunnel.

When the results of the numerical analysis are compared with the field measurements, a fair agreement is achieved. However, the shape of the vertical displacement profile computed between the tunnels, at the Trivec TR04 location is not reproduced satisfactorily. This profile exhibits an almost constant settlement for z < 19 m and a rapid decrease for distances closer to the tunnel crown level.

Finally, Figure 7 shows the normalised longitudinal settlement profile obtained from the surface monitoring point (SMP) CS12, which was installed along the MON05 array above the centreline of TBM2. This profile is shown as a function of the cutterhead's distance (x_f) from the MON05 section during the passage of TBM2. Also plotted in the same figure, in dotted form, is the cumulative probability function adopted in semi-empirical methods. This was computed under the assumption of a value of i = 0.398 (Masini and Rampello, 2021b). The results of the FE simulation are plotted in the figure as a solid line. Although the data are affected by significant scatter, surface settlements developed within the cutterhead distance range of -25 m < x_f < 35 m.

The maximum incremental settlement ($\Delta w/\Delta w_{max}$) measured at SMP CS12 was approximately 5.6 mm. The monitoring data seem to indicate that approximately 20% of vertical displacement occurs at MON05, compared to the 40% indicated by the FE analysis. These represent the upper and lower bounds of the measurements, respectively, observed for closed and open shields, respectively. However, the dispersion of the data does not permit definitive conclusions to be drawn.

5 CONCLUSIONS

The ground response observed during the excavation of the twin tunnels of the Line C of Rome underground beneath an instrumented greenfield research site was analysed using a 3D finite element model. The same set of constitutive model parameters was used in the analysis as had previously been

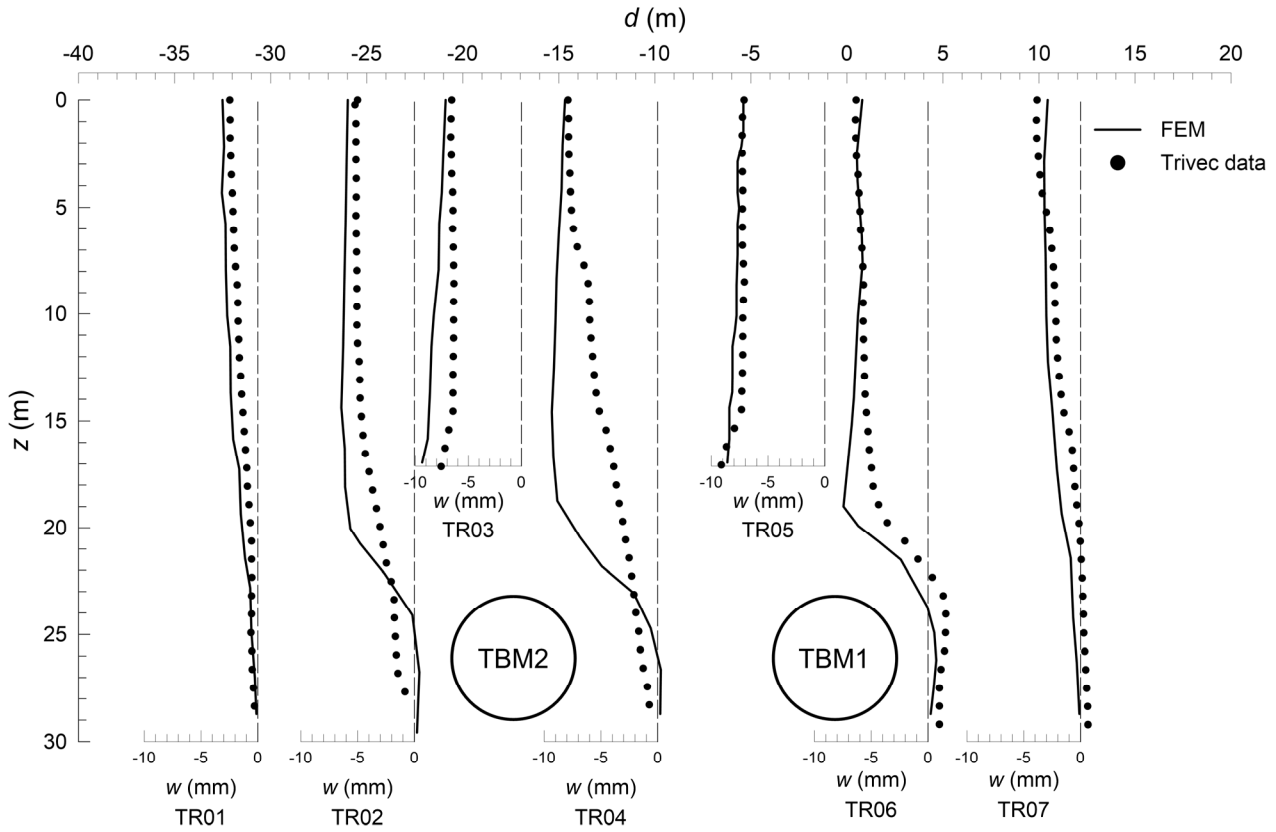

Figure 6 Vertical displacements after the passage of TBM2.

shown to successfully simulate the observed behaviour of other excavation works in the same area. These parameters were calibrated using the results of a detailed geotechnical characterisation of the site.

Investigations into the ground response to the passage of both TBMs indicate that excavating the first tunnel significantly affect the mechanical behaviour the surrounding soil, resulting in increased volume loss (+43%) and asymmetric settlement troughs. While the computed settlement profiles are in a fair agreement with the monitoring data, they highlight local deviations, especially between the tunnels, that can be attributed to uncertainties in the instrumentation. In addition, the observed longitudinal profile of the vertical displacements indicates that approximately 20% of vertical displacement occurs at MON05, compared to the 40% predicted by FE analysis but data variability prevents definitive conclusions.

These results emphasise the need to incorporate the effects of soil nonlinear and irreversible behaviour into predictive tools to reliably assess ground deformations in sequential twin tunnelling operations.

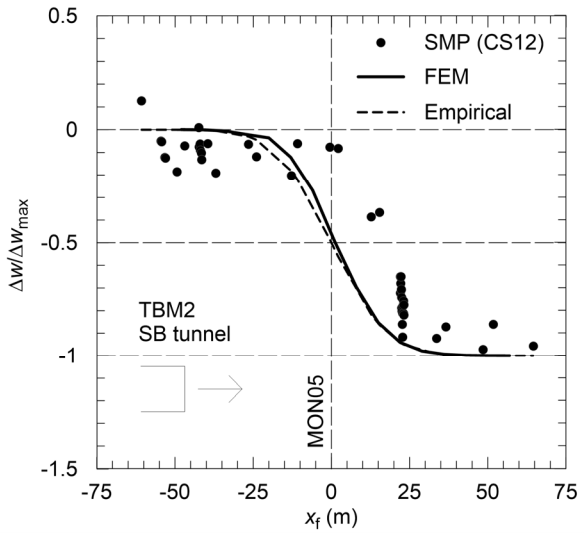

Figure 7 Longitudinal profiles of normalised incremental surface settlements during excavation of the southbound tunnel (TBM2) at SMP CS12.

6 ACKNOWLEDGEMENTS

The Authors are indebted to Metro C ScpA, particularly to Mr. Eliano Romani, for making available the monitoring data.

7 REFERENCES

Benz, T., Vermeer, P.A., and Schwab, R. 2009. A small-strain overlay model. *Int. Journal for Numerical and Analytical Methods in Geomechanics* 33, 25-44.

Brinkgreve, R.B.J., Engin, E., and Swolfs, W.M. 2013. Plaxis 3D user manual. Plaxis BV. Delft, The Netherlands.

Broere, W., and Brinkgreve, R.B.J. 2002. Phased simulation of a tunnel boring process in soft soil. *Proc. of the 5th European Conference Numerical Methods in Geotechnical Engineering NUMGE 2002*, Paris, France, 4-6 September 2002 (ed. P.Mestat). 529–536. Presses des Ponts.

Köppel, J., Amstad, C., and Kovari, K. 1983. The measurements of displacement vectors with the "TRIVEC" Borehole Probe. *Proc. of the International Symposium on Field Measurements in Geomechanics*, Zurich, (ed. K. Kovari), 1: 209-218, Balkema, Rotterdam.

Masini, L., Rampello, S., and Romani, E. 2020. Performance of a deep excavation for the new Line C of Rome underground. *In*

Geotechnical Research for Land Protection and Development – Proc. of CNRIG 2019 Springer Nature Switzerland AG 2020 F. Calvetti et al. (Eds.): CNRIG 2019, Lecture Notes in Civil Engineering (LNCE) 40: 575–582.

Masini, L., Gaudio, D., Rampello, S., and Romani, E. 2021a. Observed Performance of a Deep Excavation in the Historical Center of Rome. *Journal of Geotech. Geoenviron. Eng.* 147(2), 05020015. https://doi.org/10.1061/(ASCE)GT.1943-5606.0002465.

Masini, L., and Rampello, S. 2021b. Predicted and observed behaviour of pre-installed barriers for the mitigation of tunnelling effects. *Tunnelling and Underground Space Technology* 118, 104200.

Rampello, S., Fantera, L., and Masini, L. 2019. Efficiency of embedded barriers to mitigate tunnelling effects. *Tunnelling and Underground Space Technology* 89, 109-124. https://doi.org/10.1016/j.tust.2019.03.027

Schanz, T., Vermeer, P.A., and Bonnier, P.G. 1999. Hysteretic damping in a small-strain stiffness model. *Proc. of the 10th International Symposium on Numerical Models in Geomechanics - NUMOG 10*, London, 737-742.

Wan, M. S. P., Standing, J. R., Potts, D. M., and Burland, J. B. 2017. Measured short-term subsurface ground displacements from EPBM tunnelling in London Clay. *Géotechnique* 67(9), 748–779, http://dx.doi.org/10.1680/jgeot.SIP17.P.148.